
IFSCC 2025 full paper (IFSCC2025-243)

“Oxidation of all lipids in an artificial epidermis to model the first early events of skin aging and predictively identify active ingredients that help the skin age healthily”

Chloé Lorion¹, Amandine Lopez-Gaydon¹, Hakime Boulghobra¹, Nicolas Ritter¹, Thomas Rinaldi¹, Jean-David Rodier¹, Nicolas Bechettoille¹.

¹ R&D GATTEFOSENSE, Saint-Priest, France;

1. Introduction

Epidermal lipids are everywhere in the epidermis and their composition and organization in the skin are unique [1]. Intercellular lipids in the *stratum corneum* (SC) cover the surface of the skin and form a lipid mortar contributing to the barrier function to protect the skin from external stimuli and prevent moisture evaporation. Lipids can be defined as bioactive metabolites, crucial for the formation and function of cellular membranes, for metabolism and for cellular signaling through lipid rafts. The skin lipidome is heterogeneous and in perpetual motion; localization, function, environmental stress and age are reflected in lipid composition. Due to their unsaturated nature, epidermal lipids are the main target of oxidation in the skin, leading to their degradation by reactive oxygen species (ROS). This phenomenon of lipoperoxidation directly affects the physical properties, the integrity and function of the cell membranes within which they are formed. Lipid peroxidation produces a wide variety of oxidation products [2], like the highly reactive compound 4-Hydroxynonenal (4-HNE), the main product of pollution-driven oxidative stress considered as “one of the major toxic products generated from lipid peroxides”. As results, oxidative stress lead to loss of whole skin functions and activate signaling pathways towards inflammatory reactions [3], a natural defense system against external and internal attacks. With age or under the effect of external aggression, the inflammation

pathways are overwhelmed and contribute to chronic inflammation. In a mutual crosstalk, oxidative and inflammatory mediators feed each other, activating downstream signaling pathways related to the oxi-inflammatory phenomenon, highly harmful to skin tissue. The oxi-inflammatory damage is often associated with alteration of the skin structure and surface, commonly displayed in many skin conditions such as psoriasis and atopic dermatitis (AD) [4]. The difficulties to simulate the functional complexity of epidermal lipids and recapitulate lipid oxidation-related changes have limited the development of comprehensive and screening tools. In this context, we aimed to develop artificial epidermis models to screen a new active ingredient that will help the skin age healthily. For this purpose, we have developed *Hippophae rhamnoides* leaf ethanolic extract (*HRE*), a new strategy based on natural bioactive product for the protection of epidermal lipids.

2. Materials and Methods

2.1. Culture of reconstructed human epidermis

Keratinocytes from juvenile foreskin (< 2 years old) were seeded (2×10^5 cells/cm 2) onto Millicell® cell culture inserts, 12 mm, polycarbonate, 0.4 µm (Merck Millipore, Burlington, Massachusetts, USA) and cultured in CnT-Prime (CELLnTEC, Bern, Switzerland) at 37°C in 5% CO₂ for 3 days. Then, the system was lifted at the air-liquid interface and the culture was grown in CnT Prime Airlift medium (CELLnTEC) for 18 additional days with a change of the culture medium every 2 days.

2.2. Photo-pollution of the reconstructed human epidermis

Photo-pollution stress

First of all, urban particles matter (Standard Reference Material®, SRM 1649b, National Institute of Standards and Technology®, 50µg/cm 2) [5] were topically applied onto the surface of epidermis for 1h at 37°C in 5% CO₂. Then, epidermis with urban particles matter on their surface were irradiated in PBS with 10J/cm 2 UVA using UV system UVA 700L (Waldmann).

HRE treatment

In the preventive treatment, reconstructed epidermis were treated with the extract added in the culture medium at 0.1% for 24h and then photo-polluted according to the protocol described above. Unstressed epidermis were used as control.

In the full treatment, after a preventive treatment at 0.05%, reconstructed epidermis were treated again with the extract 0.05% for an additional 24h and then photo-polluted according to the protocol described above. A last treatment with the extract 0.05% was applied for additional 6h. Unstressed epidermis were used as control.

2.3. In-house pollution box

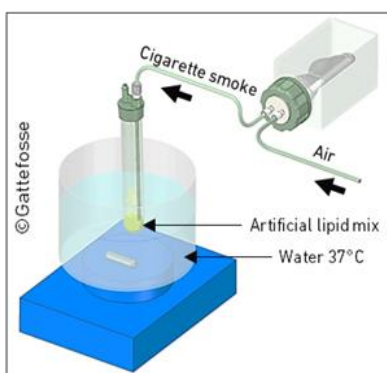


Figure 1. In-house pollution box allowing oxidation of artificial lipid mix by cigarette smoke. The pollution box worked as follows: The lipid mix, contained in a closed tube, was maintained at 37°C in a water bath with stirring. In parallel, 2 cigarettes were placed in a closed chamber. To activate oxidation, air was injected into the cigarette chamber at a controlled flow rate (10L/h) to ensure their consumption. The condensate of cigarette smoke thus formed then passed into the tube containing the lipid mix, this for 8 hours.

2.4. Flow cytometry assay

The secretion of interleukin-1alpha (IL-1 α), interleukin-8 (IL-8) and interferon-gamma (IFN- γ) pro-inflammatory cytokines was quantified in culture supernatants of reconstructed epidermis treated or not with the oxidized lipid mix, using LEGENDplex-Custom Human 13-plex Panel (BioLegend, San Diego, CA, USA). Unstressed epidermis were used as control. Results were expressed as the % of IL-1 α , IL-8 or IFN- γ secretion vs. oxidized lipid mix. Data were expressed as mean \pm SD. Three independent experiments were performed in duplicate ($n=2$). The statistical analysis was performed vs. the oxidized lipid mix condition: 1 Way-ANOVA followed by Tukey's multiple comparisons test.

2.5. Lucifer yellow (LY) permeability assay

Reconstructed epidermis samples were loaded with 150 μ l of LY dye solution 1mM (Thermo Fisher Scientific) and incubated for 1 hour at 37°C before being rinsed in phosphate buffered saline and processed for fluorescence analysis. Samples were embedded in Tissue Tek OCT compound (Microm Microtech) and frozen sections (10 μ m) were cut, placed onto Superfrost Gold plus (DUTSHER, Bernolsheim, France) slides and fixed with cold acetone for 10 minutes. The mounting medium (Prolong Gold antifade reagent, Thermo Fisher Scientific) contained DAPI for nucleus staining. Fluorescent staining was observed using an Axio Imager M2 fluorescence microscope (Zeiss) and quantified (area of ROI) using Zen image analysis software (Zeiss). Unstressed epidermis were used as control.

3. Results

3.1. Modeling the peroxidation of skin lipids in viable epidermis and protection with the *HRE*

We used a 3D model of reconstructed human epidermis stressed by photo-pollution to study the lipid peroxidation in keratinocyte cell membranes. Exposure of urban particle matters combined with UVA irradiation induced a high expression of 4-HNE expression in all viable layers of epidermis (Figure 2.a). It is noteworthy that 4-HNE expression in photo-polluted epidermis treated in preventively and curatively by the *HRE* was approximately equivalent to that found in the control. 4-HNE expression was significantly increased by +84% \pm 15% ($p<0.001$) in photo-polluted epidermis (Figure 2.b), while in the *HRE* preventive treatment (0.1%), it was reduced by 33% \pm 15% ($p<0.001$) and even up to 68% \pm 14% ($p<0.001$) in preventive and curative treatment (0.05%), thus suggesting a dose-effect. Thanks to its antioxidant properties, the *HRE* could protect keratinocyte cell membranes from lipoperoxidation in epidermis challenged by photo-pollution insults.

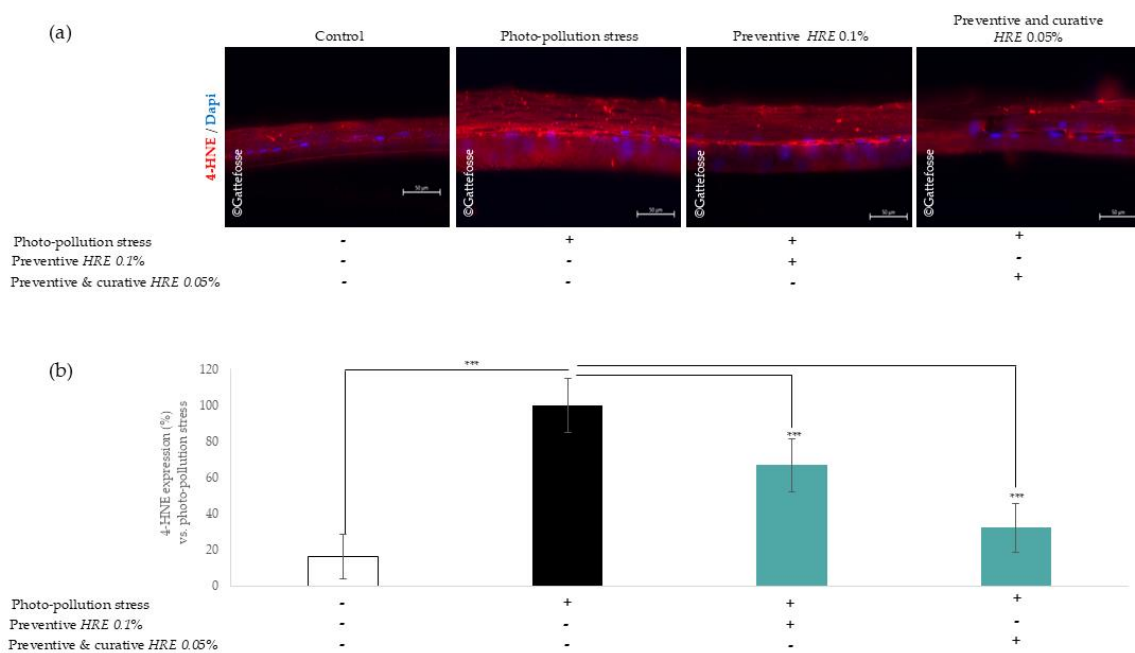


Figure 2. The HRE protected lipids of keratinocyte cell membranes from lipoperoxidation. (a) Immunofluorescence imaging of 4-HNE expression (red) in photo-polluted epidermis treated with the HRE in preventive at 0.1% and in preventive and curative at 0.05%. DAPI (blue) was used for nuclear staining. Unstressed epidermis were used as control. Scale bar = 50µm. (b) Immunofluorescence image analysis of 4-HNE expression. The representative data were shown as mean ± SD, in % relative to photo-pollution stress, from three independent experiments with an analysis of three images per experiment (n=3). The statistical analysis was performed vs. the photo-pollution stress condition: Two Way-ANOVA followed by Dunnett's multiple comparisons test; *** p<0.001.

3.2. Modeling the oxidation of skin lipids in the SC of epidermis and protection against inflammation with the HRE.

From the lipid mixture proposed by Le Cui *et al.*, [6], we developed a complex artificial lipid mix, which is representative of lipids found in normal human skin, except the ceramides (Table 1).

| Cui et al., (Journal of Cosmetic Dermatology, 2016) | Artificial Lipid mix | | |
|---|----------------------|--------|----------------|
| | % mass | % mass | composition |
| Free fatty acids | 16.4 | 16 | Oleic acid |
| Triglycerides | 41 | 42 | Triolein |
| Wax esters | 25 | 26 | Oleyl stearate |
| Squalene | 12 | 12 | Squalene |
| Cholesteryl esters | 2.1 | 0 | / |
| Cholesterol (CHO) | 1.4 | 4 | Cholesterol |

Table 1. Composition and % mass of artificial lipid mix.

Using in-house engineering system, we oxidized the lipid mixture with a smoke condensate of standardized cigarettes (3R4F, University of Kentucky, UK), which contain defined amounts of particles, tar, nicotine and carbon monoxide to mimic pollution stress.

The oxidized state of lipid mixture was confirmed by its peroxide index around 14.68 meq O₂/kg (compared to the control mix at 1.62 meq O₂/kg) and GC-MS chromatography showing volatile compounds of the benzene and styrene type or pyridine derivatives (Figure 3).

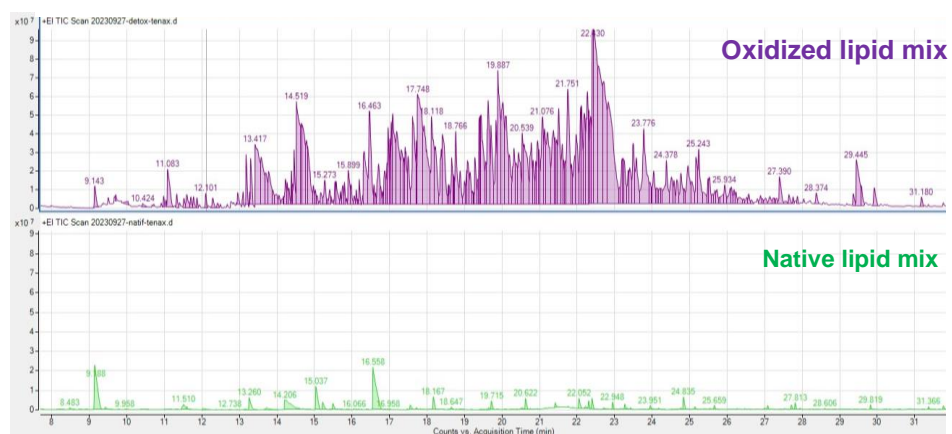


Figure 3. Analysis of volatile compounds by GC-MS chromatography. Analysis of volatile compounds by GC-MS chromatography confirmed also the oxidized state of lipids in the mix. In the oxidized lipid mix, many volatile compounds that have been in contact with cigarette smoke vapors were clearly highlighted compared to the native lipid mix.

To model the oxi-inflammation in the SC, we developed a study model in which the artificial mix of lipids, oxidized or not is topically applied on the surface of a reconstructed human epidermis for 48h (Figure 4). Non-oxidized lipid mix had no effect on the epidermis, which exhibited a proper epidermal morphology. In contrast, pyknotic nuclei were found within the epidermis to which oxidized lipid mix was topically applied. Even epidermis treated by the *HRE* 0.1% for 48h and then stressed by the oxidized lipid mix still showed pyknotic nuclei within the tissue. At histological level, the *HRE* therefore did not seem to protect epidermis against damage induced by oxidized lipids.

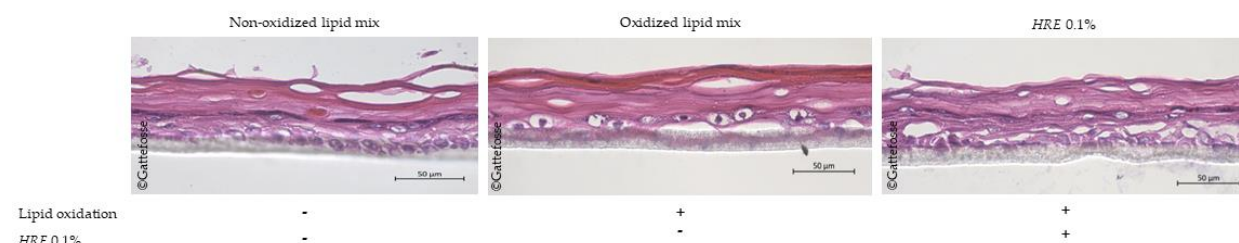


Figure 4. The HRE did not protect epidermis against damage induced by oxidized lipids. Hematoxylin-eosin staining of reconstructed epidermis treated in preventive with the *HRE* at 0.1% for 48h and then stressed by the oxidized lipid mix for an additional 48h. Scale bar= 50 μ m.

We also quantified IL-1 α , IL-8 and IFN- γ pro-inflammatory cytokines secreted in culture supernatants using flow cytometry. As expected, oxidized lipid mix triggered a huge release of IL-1 α (Figure 5.a), IL-8 (Figure 5.b) and IFN- γ (Figure 5.c) compared to the non-oxidized lipid mix, thus highlighting the oxi-inflammation phenomenon. Interestingly, the *HRE* significantly inhibited the secretion of IL-1 α (-56% \pm 13%, p<0.001), IL-8 (-66% \pm 21%, p<0.01) and IFN- γ (-57% \pm 9%, p<0.0001) in epidermis to which oxidized lipid mix were applied. With the *HRE* treatment, epidermis to which oxidized lipid mix were applied now exhibited a cytokine secretion close to that found in epidermis with the non-oxidized lipid mix. Taken together, the *HRE* could decrease the inflammatory response in the epidermis induced by oxidation of lipids in the SC.

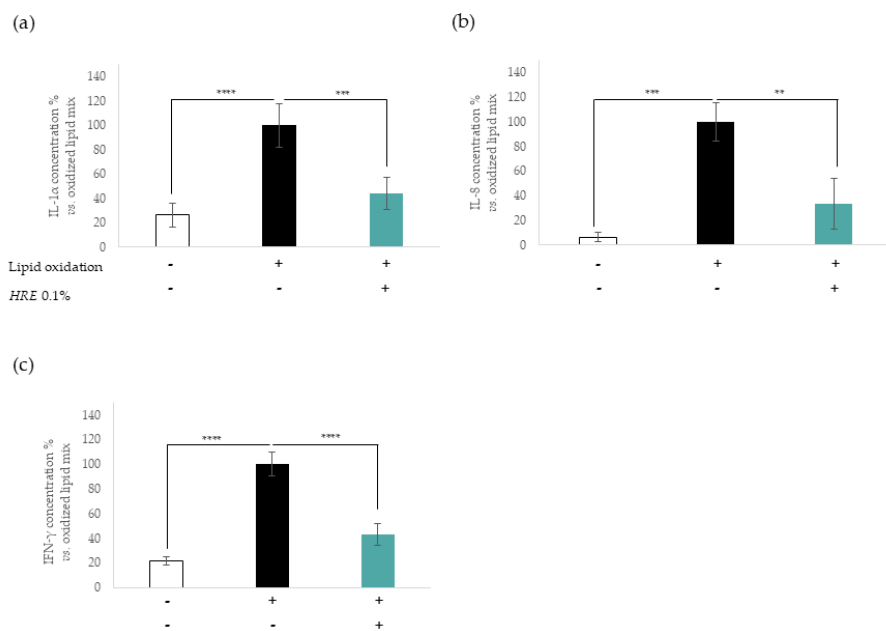


Figure 5. The HRE reduced the secretion of pro-inflammatory cytokines induced by oxidation of lipids in the SC. (a) IL-1 α (a), IL-8 (b) and IFN- γ (c) quantification (%) vs. the oxidized lipid mix in culture supernatants of reconstructed epidermis treated in preventive with the *HRE* at 0.1% for 48h and then stressed by the oxidized lipid mix for an additional 48h. Unstressed epidermis were used as control. The representative data were shown as mean \pm SD from three independent experiments in duplicate (n=2). The statistical analysis was performed vs. the oxidized lipid mix condition: 1 Way-ANOVA followed by Tukey's multiple comparisons test; **** p<0.0001; *** p<0.001 and ** p<0.01.

3.3. Improvement of skin barrier function with the *HRE*.

A defective skin barrier, such as that found in AD and eczema, results from altered lipid structures in the SC and a chronic inflammatory state of the epidermis. We therefore examined whether the *HRE* was also able to strengthen the skin barrier function. For this, we used the 3D model of reconstructed human epidermis stressed by photo-pollution, as previously used to study lipoperoxidation. Exposure of urban particle matters combined with UVA irradiation impaired the barrier function of epidermis, as shown by diffuse LY staining in the tissue (Figure 6). Interestingly, the LY dye in the photo-polluted epidermis treated preventively with the *HRE* remained localized in the SC as in the control condition.

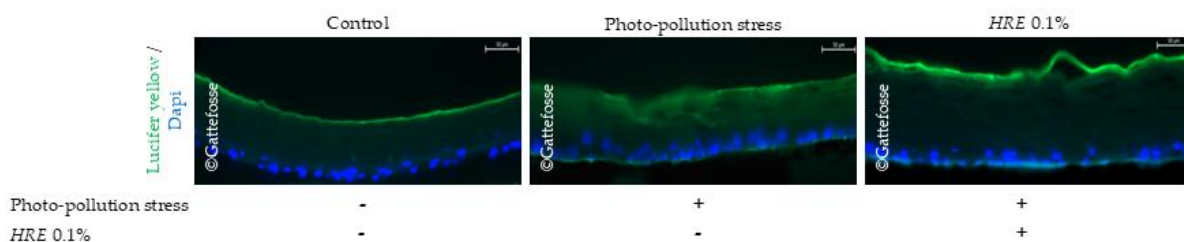


Figure 6. The *HRE* reinforced the skin barrier function. Diffusion of the Lucifer Yellow (LY) fluorescent dye (green) was used to visualize the permeability of reconstructed epidermis treated in preventive with the *HRE* at 0.1% for 24h and then stressed with photo-pollution (SRM 1649b 50 μ g/cm 2 and UVA 10J/cm 2). Unstressed epidermis were used as control. DAPI (blue) was used for nuclear staining. Scale bar = 50 μ m.

4. Discussion

In the epidermis, the lipidome is central to healthy and radiant skin. Lipids are required for the maintenance and regulation of the epidermal barrier, skin homeostasis, physical properties of the skin and defense against microbes. Many factors contribute to variability in the skin lipidome, such as age, sex, body part, pigmentation, and depth of skin sampling. Therefore, in skin care products, special attention should be given to the protection of epidermal lipids against exposome factors. In our study, we have developed artificial epidermis models that mimic lipids oxidation and inflammation exacerbated by extrinsic factors and we investigated the potential cosmetic benefits of the *HRE* to protect epidermal lipids against oxi-inflammatory environment.

The potential antioxidant properties of the *HRE* were confirmed in a more predictive model of reconstructed human epidermis stressed by photo-pollution, to analyze the rate of lipid peroxidation in keratinocyte cell membranes. Recent works demonstrated the interplay between pollution and UVA in the disturbance of skin redox homeostasis, inflammation and barrier function alteration, resulting in oxi-inflammation [7]. To study lipoperoxidation in skin models, photo-pollution represents the reference stress to evaluate the efficacy of an active ingredient on the protection of membrane lipids against oxidation [8]. Indeed, the lipid rich components of the epidermis are targets of pollution and sun radiation. Lipid peroxidation is an early event in chronic skin inflammatory diseases: psoriasis [3], AD [9] and acne vulgaris [10]. We highlighted that the *HRE* significantly inhibited IL-1 α , IL-8 and IFN- γ pro-inflammatory cytokines in a reconstructed epidermis model to which an oxidized lipids mix was applied. In the composition of the artificial lipid mix, we did not included ceramides despite their crucial role as a water impermeable barrier and their involvement in the dysfunction of SC in aged skin and some cutaneous inflammatory diseases such as AD and psoriasis. Even if the main components of the SC lipid matrix are well-known, the exact composition and molecular landscape of the SC lipid matrix is continually being updated and refined through ongoing research. Besides, ceramides are not described as the first targets of oxidation lipids. The artificial lipid mix was oxidized by a condensate of cigarette smoke which is the reference stress model to study the oxidation of lipids in the SC [11]. The oxi-inflammatory damage is often associated with alteration of the skin structure and surface, which leads to a defective skin barrier due to degraded lipid structures in the SC, commonly displayed in psoriasis and AD [12]. We highlighted that the *HRE* fully protected the barrier function of epidermis against photo-pollution insults.

To go further, the *HRE* was clinically proven to soothe reactive and sensitive skin, with reduced redness and imperfections, and to help skin regain glow and comfort, even under harsh conditions skin (data not shown).

5. Conclusion

These results clearly highlight that knowledge from skin lipidomics can thus improve our understanding of skin health, diseases and responses to environmental factors to combat oxi-

inflammation. *Hippophae rhamnoides* leaf extract treatment exerted a beneficial and pro-health effect on the skin by protecting cutaneous lipids from external aggressions through the stimulation of antioxidant defenses and the inhibition of pro-inflammatory signaling pathways.

References

1. Knox, S.; O'Boyle, N.M. Skin lipids in health and disease: A review. *Chem. Phys. Lipids* **2021**, *236*, 105055, doi:10.1016/j.chemphyslip.2021.105055.
2. Ayala, A.; Muñoz, M.F.; Argüelles, S. Lipid peroxidation: production, metabolism, and signaling mechanisms of malondialdehyde and 4-hydroxy-2-nonenal. *Oxid. Med. Cell. Longev.* **2014**, *2014*, 360438, doi:10.1155/2014/360438.
3. Wroński, A.; Gęgotek, A.; Skrzypieńska, E. Protein adducts with lipid peroxidation products in patients with psoriasis. *Redox Biol.* **2023**, *63*, 102729, doi:10.1016/j.redox.2023.102729.
4. Valacchi, G.; Virgili, F.; Cervellati, C.; Pecorelli, A. OxInflammation: From Subclinical Condition to Pathological Biomarker. *Front. Physiol.* **2018**, *9*, 858, doi:10.3389/fphys.2018.00858.
5. Pan, T.-L.; Wang, P.-W.; Aljuffali, I.A.; Huang, C.-T.; Lee, C.-W.; Fang, J.-Y. The impact of urban particulate pollution on skin barrier function and the subsequent drug absorption. *J. Dermatol. Sci.* **2015**, *78*, 51–60, doi:10.1016/j.jdermsci.2015.01.011.
6. Le Cui; Jia, Y.; Cheng, Z.-W.; Gao, Y.; Zhang, G.-L.; Li, J.-Y.; He, C.-F. Advancements in the maintenance of skin barrier/skin lipid composition and the involvement of metabolic enzymes. *J. Cosmet. Dermatol.* **2016**, *15*, 549–558, doi:10.1111/jocd.12245.
7. Soeur, J.; Belaidi, J.-P.; Chollet, C.; Denat, L.; Dimitrov, A.; Jones, C.; Perez, P.; Zanini, M.; Zobiri, O.; Mezzache, S.; et al. Photo-pollution stress in skin: Traces of pollutants (PAH and particulate matter) impair redox homeostasis in keratinocytes exposed to UVA1. *J. Dermatol. Sci.* **2017**, *86*, 162–169, doi:10.1016/j.jdermsci.2017.01.007.
8. Larnac, E.; Montoni, A.; Haydout, V.; Marrot, L.; Rochette, P.J. Lipid Peroxidation as the Mechanism Underlying Polycyclic Aromatic Hydrocarbons and Sunlight Synergistic Toxicity in Dermal Fibroblasts. *Int. J. Mol. Sci.* **2024**, *25*, doi:10.3390/ijms25031905.
9. Niwa, Y.; Sumi, H.; Kawahira, K.; Terashima, T.; Nakamura, T.; Akamatsu, H. Protein oxidative damage in the stratum corneum: Evidence for a link between environmental oxidants and the changing prevalence and nature of atopic dermatitis in Japan. *Br. J. Dermatol.* **2003**, *149*, 248–254, doi:10.1046/j.1365-2133.2003.05417.x.
10. Bowe, W.P.; Patel, N.; Logan, A.C. Acne vulgaris: the role of oxidative stress and the potential therapeutic value of local and systemic antioxidants. *J. Drugs Dermatol.* **2012**, *11*, 742–746.
11. Hergesell, K.; Paraskevopoulou, A.; Opálka, L.; Velebný, V.; Vávrová, K.; Dolečková, I. The effect of long-term cigarette smoking on selected skin barrier proteins and lipids. *Sci. Rep.* **2023**, *13*, doi:10.1038/s41598-023-38178-7.
12. Ferrara, F.; Woodby, B.; Pecorelli, A.; Schiavone, M.L.; Pambianchi, E.; Messano, N.; Therrien, J.-P.; Choudhary, H.; Valacchi, G. Additive effect of combined pollutants to UV induced skin Ox-Inflammation damage. Evaluating the protective topical application of a cosmeceutical mixture formulation. *Redox Biol.* **2020**, *34*, 101481, doi:10.1016/j.redox.2020.101481.